SELECTION OF WORKING FLUID AND EXERGY ANALYSIS OF AN ORGANIC RANKINE CYCLE

Aseem Desai[1], Deepa Agrawal[2],

Sauradeep Datta[3], Sanjay Rumde[4]

[1,2,3,4] *Mechanical Engineering Department, Maharashtra Institute of Technology (India)*

ABSTRACT

There are two degrees of freedom available in designing an Organic Rankine Cycle (O.R.C) - the organic fluid and the evaporator pressure. The upper limit of the latter will be decided by the heat source inlet temperature. The performance of 12 organic fluids including some newly developed silicone oils - D4, MDM, have been analyzed on the basis of thermal efficiency, exergy destruction (neglecting pressure drop) and size of the system required. The optimum evaporator pressure was found for each fluid using power output as the objective function. The source was taken as a flue gas mixture at 150˚C. The exergy destruction due to two irreversibility –heat transfer across a finite temperature difference and pressure drop in a shell and tube heat exchanger was quantified only for R245fa and recalculated for varying source exit temperature. The average tube side heat transfer coefficient and that for liquid-only were obtained from HTRI software for a given geometry. The pressure drop in the shell was obtained using Bell-Delaware method and that in the tube was calculated separately for the single phase and two phase part.

Keywords: Evaporator, Exergy analysis, Organic Rankine Cycle

I. INTRODUCTION

The need for better efficiencies in power plants has never been greater. With drastic climate change occurring all over the world, we need to reduce dangerous emissions into the atmosphere. More than 50% waste heat is unused; converting some of this heat into work can attenuate the problem by reducing the consumption of fossil fuels [1]. Another solution to this problem is the use of renewable sources of energy, like solar and geothermal, which are low grade heat sources. The operation at lower temperatures requires an organic fluid in the power cycle. Organic fluids have much lower normal boiling point than water hence is suitable for low temperature applications. Also organic fluids have lower specific volume as compared to steam hence the corresponding size of the components of the power plant will be considerably smaller.

The importance of exergy is often ignored but as per the Carnot corollary, maximum work is developed only when the irreversibility's are eradicated. Increasing the exit temperature of the source increases the Log Mean Temperature Difference (LMTD) in the evaporator and hence reduces its size. The reduced size and mass flux should give lower pressure drop. Hence, while the exergy destruction due to the temperature difference increases with increase in source exit temperature, the pressure drop irreversibility reduces with the same [2].

| Nomenclature		Subscripts	
Q	heat transfer rate (KW)	1,2,2s,3,4,4s,5,6,7,8	states in system
$\dot{m}_h$	mass flow rate of hot fluid (kg/s)	e	evaporator
$\dot{m}_c$	mass flow rate of hot fluid (kg/s)	c	condenser
$\dot{m}_{cw}$	mass flow rate of cooling water(kg/s)	p	pump
h	enthalpy (KJ/kg)	LO	liquid only
S	entropy (KJ/kgK)	g	flue gas
η	efficiency	l	liquid refrigerant
W	work energy (KJ)		
T	temperature (˚C)		
T_o	surrounding temperature		
Φ	heat Recovery Efficiency		
Δ	finite change in quantity		
P	pressure (Pa)		
N_b	number of baffles		
μ	viscosity (Pa-s)		
ρ	mean density (kg/m^3)		
$ρ_i$	density at inlet (kg/m^3)		
$ρ_o$	density at outlet (kg/m^3)		
G	mass flux (kg/m^2)		
l	length of tube (m)		
r_h	hydraulic radius (m)		
X_{LM}	Lockhart-Martinelli parameter		
N	number of tubes in evaporator		
U_{avg}	overall heat transfer coefficient		
d_o	outer diameter of tube		
T_{exit}	flue gas exit temperature		
C_{ph}	specific heat at constant pressure for hot fluid (KJ/kgK)		
A_s	surface area of evaporator		
$\dot{I}$	exergy destruction rate (KW)		
x	dryness fraction		
f	friction factor		
Re	Reynolds Number		
Cf	correction factor		
Nu	Nusselt number		
Pr	Prandtl number		

Another factor is the heat transfer coefficient whose variation may have a drastic effect on the size of the heat exchanger and hence on the exergy destruction.

Many researches have worked on fluid selection for an ORC, Hung et al [3] found the thermal efficiencies of Benzene, Toluene, p-xylene, R113 and concluded that p-xylene had the maximum and benzene has the minimum efficiency. He also found that p-xylene had the lowest overall irreversibility and that maximum irreversibility was present in the evaporator. Wang et al [1] conducted a multi-objective optimization considering heat exchanger surface area per unit power output and the heat recovery efficiency and surmised that R141b is the optimal fluid if the source inlet temperature is greater than $180\,^{\circ}$C. Lars et al [4] considered the variation of thermal efficiency with critical temperature and found that they had an increasing relationship. Dai et al [5] showed that R236ea had the highest exergy efficiency and that for fixed input source conditions, the maximum power is obtained at a certain optimum evaporator pressure. Larjola et al [6] showed that for a larger two-phase enthalpy drop in the evaporator, the irreversibility in it will be greater. Wei et al [7] analyzed the effect of variation in source parameters like mass flow rate and inlet temperature of the exhaust of an IC engine, on the exergy destruction and thermal efficiency for R245fa.

In this study the fluid selection and exergy analysis (neglecting pressure drop in the evaporator) has been extended to some more fluids like D4, MDM, and R141b etc. The fluids containing chlorine have not been considered in this paper due to their high ODP. In addition the exergy destruction due to pressure drop in a shell and tube heat exchanger was also considered for R245fa. The occurrence of a trade-off has been checked for the given source conditions. The exit temperature of the source was varied and the corresponding exergy destruction in the evaporator was plotted. The effect of increasing the temperature difference between hot and cold fluids in the heat exchanger, on the heat transfer coefficient and size is also shown.

II. MODEL OF AN ORGANIC RANKINE CYCLE

Schematic diagram of the organic rankine cycle as shown in fig. 1 consists of an evaporator driven by low-grade heat source, an expander, a condenser and a working fluid pump. The working fluid is pumped into the evaporator where it is heated and vaporised by the waste heat. The high pressure vapour enters the expander without any superheat, where the vapour gets expanded and power is generated. After this the exhaust vapour enters the condenser while it is still in the superheated state, where it gets condensed by cooling water and then it is pumped back to the evaporator and a new cycle begins.
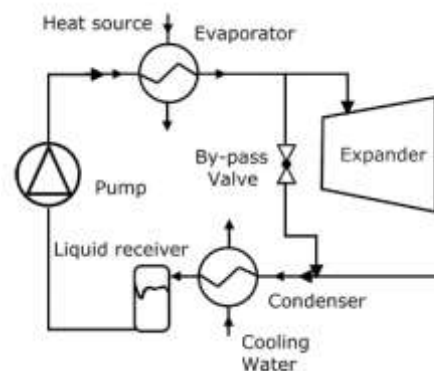
Fig. 1. Schematic diagram of ORC

2.1 Source and Sink Conditions

The waste heat source considered here is a flue gas mixture. The flue gas inlet temperature is assumed constant at 150˚C. A constant pinch of 7˚C was taken between the hot and cold fluid at the point at which two phase flow begins on the cold side. The condenser temperature is kept constant at 50˚C. Since pinch of 5˚C is maintained, cooling water exit temperature is taken as 45˚C. Due to limitations of the cooling tower the cooling water inlet is kept at 35˚C.

2.2 Thermodynamic Analysis

The thermodynamic processes involved in a basic subcritical ORC are illustrated in fig. 2. 1-2 and 3-4 (represented by dotted lines) indicate the actual processes, whereas 1-2s and 3-4s indicate the ideal reversible processes.

Process 4-1: This process represents a constant pressure heat addition in evaporator. The heat absorbed by working fluid in the evaporator is:

$$\dot{Q}_e = \dot{m}_h (h_5 - h_6) = \dot{m}_c (h_1 - h_4) \tag{1}$$

Process 1-2: The high pressure vapour working fluid from the evaporator enters the expander where mechanical power is developed. Power developed by the expander is:

$$\dot{W}exp = \dot{m}_c (h_1 - h_{2s}) \eta_e \tag{2}$$

Expander efficiency (η_e) has been assumed as 70%.

Process 2-3: This process represents a constant pressure heat rejection in condenser. The heat rejected by the working fluid in the condenser is:

$$\dot{Q}c = \dot{m}_c (h_2 - h_3) \tag{3}$$

Process 3-4: This process indicates actual pumping process. The power consumed by the pump is:

$$\dot{W}_p = \frac{\dot{m}_c (h_{4s} - h_3)}{\eta_p} \tag{4}$$

The pump efficiency (η_p) has been assumed to 60%.
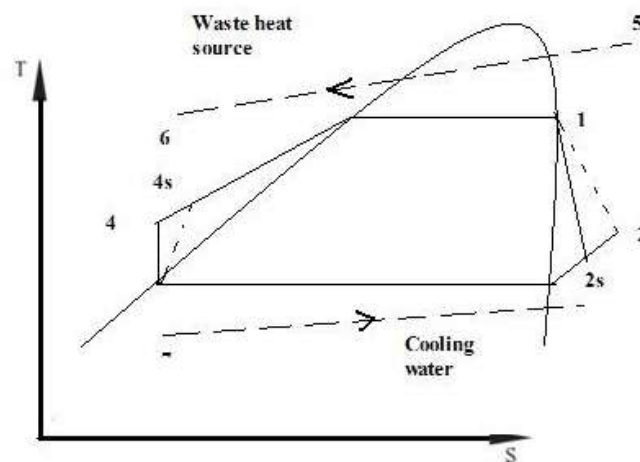

Fig. 2. T-S diagram of ORC system with heat source and cooling water

2.3 Selection of Working Fluid

Selection of correct working fluid is a very important aspect to be considered before designing the ORC. Organic fluids have lower normal boiling points and hence have very high pressures at moderate temperatures facilitating a positive pressure difference in the evaporator. The higher pressure also results in lower specific volumes and hence smaller size of the components. The fluid must also be selected on the basis of the source conditions, as the critical temperature of the fluid may be much smaller or larger than the source temperature.

One of the important thermodynamic attributes of the organic fluid is the slope of the saturation vapour curve. On this basis organic fluids are classified into dry, wet and isentropic fluids. For dry fluids, the slope of the saturated vapour line is positive. Some examples of dry fluids are R245fa, isobutene, R141b, toluene, p-xylene. For wet fluids, the slope of the saturated vapour line is negative. Some examples of wet fluids are water, ethanol, R152. For isentropic fluids, the slope of the saturation vapour curve is infinity. Some examples of isentropic fluids are R134a, R125, R245ca.

Due to the negative slope of saturated vapour curve of the wet fluids in the T-S diagram, the exit state of the fluid from the turbine is often wet. This problem is eliminated for organic fluids since at the exit of the turbine the fluid is always superheated. Another benefit is that the exit temperature of the fluid from the turbine is usually higher than that of the fluid at the exit of the pump. Hence there is some scope for improving the efficiency by introducing regeneration. Unlike the wet fluids no bleed is required from the turbine and hence he fluid expands completely in the turbine. The performance of fluids is evaluated based on three parameters: Thermal efficiency, Maximum power output, Exergy destruction.

2.3.1 Thermal Efficiency Analysis of Various Working Fluids

The thermal efficiency for various working fluids has been calculated based on the thermodynamic model describe previously, using a Matlab program. The fluid properties were obtained by using REFPROP (9.1) software which was linked with Matlab. In this text evaporator temperature refers to the temperature at which boiling starts (T_1, T_9).
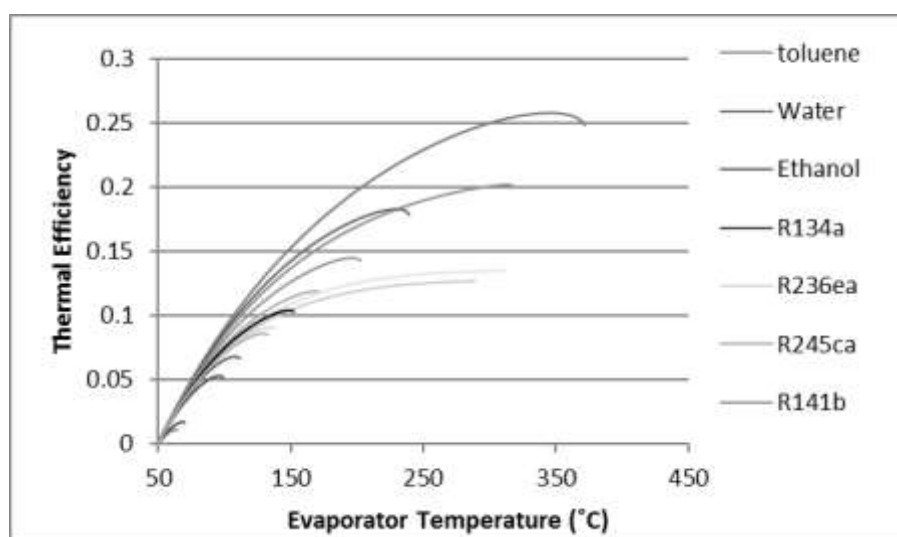

Fig. 3. Thermal efficiency of various fluids plotted against evaporator temperature (at which boiling starts) varying from 50˚C up to the critical temperature of particular working fluid

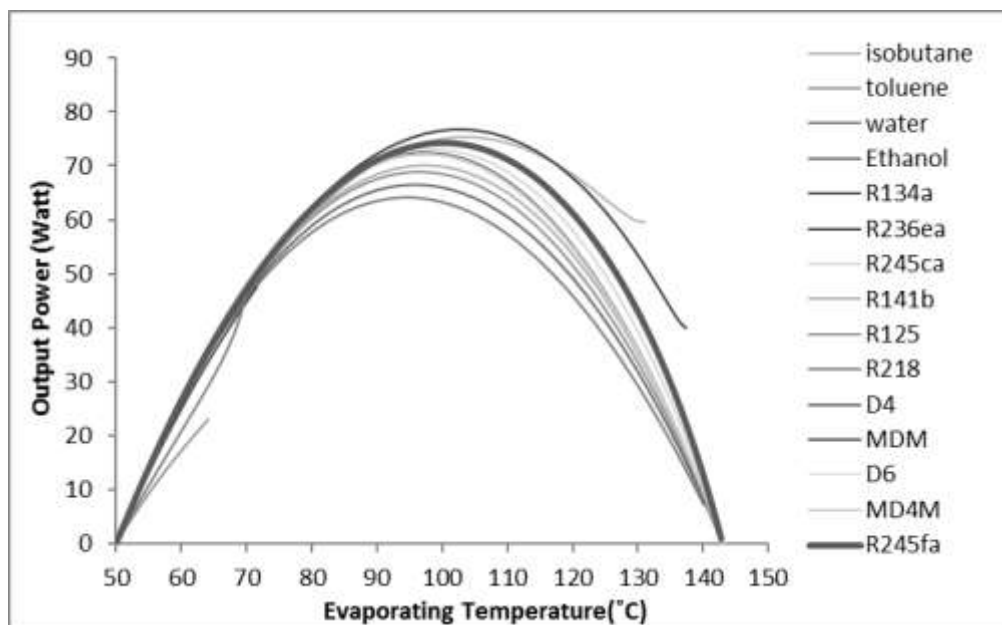### 2.3.2 Analysis of Maximum Power Output for various working fluids

The evaporator temperature adds a restriction on the lowest possible heat source exit temperature. This is because the maximum temperature difference at pinch point is taken as 7˚C. For an ORC, the pinch point is the point at which evaporation begins or the point at which dryness fraction is zero.

The net power output is a product of thermal efficiency and heat duty. As evaporator temperature increases thermal efficiency increases and simultaneously heat duty decreases. Hence it is required to find the evaporator temperature corresponding to which maximum power output is obtained. As the evaporator temperature increases the heat recovery efficiency decreases.

Heat recovery efficiency (Ø) is the ratio of the available energy to the maximum usable energy.

$$\emptyset = \frac{(T5 - T6)}{(T5 - T4 - \Delta TP)} \tag{5}$$

As heat recovery efficiency increases thermal efficiency decreases. Thus, the thermal efficiency and heat recovery efficiency are inversely related.

Fig. 4. Shows the variation of output power with change in evaporator temperature for various working fluids

The power output for various working fluids has been calculated using a Matlab program and the temperature for maximum power has been noted.

2.3.3. Exergy Analysis for Entire Cycle

Exergy refers to the total available energy. The efficiency is not an accurate parameter for defining the maximum power producing capacity of an ORC. For this, we need to quantify the irreversibility's by using the exergy destruction. In each of the 4 components, there is some irreversibility.

The exergy destruction is always equal to product of net entropy generation rate and surrounding temperature.

$$I = \dot{S}_{gen} T_o \tag{6}$$

- In the evaporator, there is an exchange of heat between a finite temperature difference (Flue gas and Organic fluid), ideally another heat engine could be added between these two temperature source and sink, and more work could be extracted. The drop in pressure due to friction in the pipes also results in some work lost in fighting friction.

$$I_{evap} = (\dot{m}_h(S2 - S6) + \dot{m}_c(S4 - S1))T_0 \qquad (7)$$

- Similarly the friction between viscous fluid and blades in the turbine also results in some work lost.

$$I_{turb} = \dot{m}_c(S2 - S2s)T_0 \qquad (8)$$

- In the condenser, there is net entropy generation due to heat transfer across a finite temperature difference, this time between the organic fluid and cooling water.

$$I_{cond} = (\dot{m}_{cw}(S7 - S8) + \dot{m}_c(S2 - S3))To \qquad (9)$$

- Finally the friction between the impeller blades in the pump and the organic fluid results in some entropy generation.

$$I_{pump} = \dot{m}_c(S4 - S4s)T_0 \qquad (10)$$

The exergy destruction is defined as the product of environment temperature and the net entropy generation. The net entropy generation is calculated in each component after assuming suitable isentropic efficiencies in the turbine and pump. The pressure drop in the heat exchangers is neglected.

$$I_{total} = I_{pump} + I_{turb} + I_{evap} + I_{cond} \qquad (11)$$

As the evaporator temperature increases, the total exergy destruction decreases because the temperature difference between the heat source and the organic fluid reduces along with the mass flow rate of organic fluid in the cycle. Unfortunately the total heat recovered from the source also reduces. Hence lower irreversibility will be obtained at the cost of lower heat recovery efficiency and lower power developed. It can also be concluded that for fluids with higher critical temperature, the two phase enthalpy drop is larger and so is the exergy destruction in the evaporator, yet since the LMTD is larger, a smaller heat exchanger required.
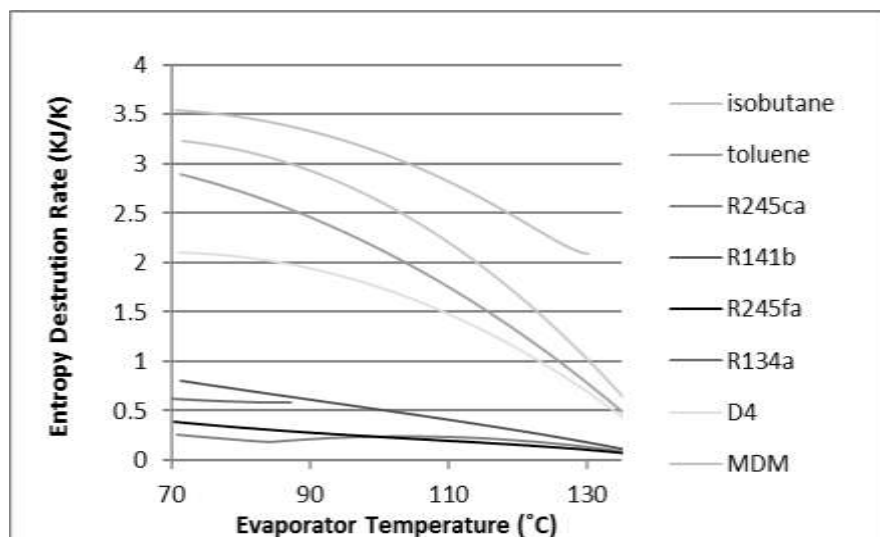

Fig. 5. Represents the overall entropy destruction rate as a function of evaporator temperature for various organic fluids.

Table 1 shows the maximum power output and thermal efficiency for the various working along with certain thermo-physical property

Fluids	Molecular Weight (g/mol)	Slope of Saturated vapour Line $(\frac{dT}{dS})$	Critical Pressure (bar)	Critical Temperature (°C)	Specific Volume at intermediate temperature of 85°C (m³/kg)	Overall Thermal Efficiency for Te=120°C And Tc=50°C (%)	Maximum Power output (KW)	Evaporator Temperature at which power is maximum
Water	18.0153	Negative	220.64	373.95	0.1	24.88	64.25	95.07
Isobutane	58.12	Positive	36.29	134.66	0.0262	8.47	75.43	103.729
R245fa	134.05	Positive	36.51	154.01	0.0242	10.35	74.36	99.98
MDM	193.24	Positive	14.15	290.94	0.33	12.72	72.43	97.788
D4	296.62	Positive	13.32	313.34	0.58	13.49	72.22	97.04
R134a	102	Isentropic	37.61	72.71	0.0064	5.26	108.83	99.06
R141b	117	Positive	42.12	204.35	0.0617	14.34	70.02	97.22
R125	120	Isentropic	36.18	66.02	0.0025	1.07	23.15	64.023
R245ca	134.05	Isentropic	39.41	174.42	0.0478	11.78	73.07	98.968
Toluene	92.14	Positive	41.26	318.60	0.4340	20.17	68.82	95.322
R152a	66.1	Negative	45.17	113.26	0.0121	6.63	104.11	111.261
R236ea	152.03	Negative	34.2	139.29	0.0155	8.98	76.87	102.374

III. MODEL OF EVAPORATOR

The evaporator considered is a shell and tube heat exchanger. The working fluid flows through the tubes and the flue gas flows through the shell enclosure. The shell diameter and corresponding tube count has been selected by using 'Heat Transfer Research, Inc. (HTRI)' software after supplying the process condition which includes the constant evaporator temperature of 120°C. The shell Diameter was taken as 1150 mm, with a pitch of 25 mm for a 45° staggered tube configuration, the tube count was 728. The tube diameter was taken as 19 mm and thickness as 1.5mm. The shell type was 'E', Front End-'B', Rear End-'S' and the baffle spacing was taken as

330mm. The source exit temperature was varied from 127°C up to 147°C. The corresponding overall heat transfer coefficient and the liquid-only heat transfer coefficient was also obtained from HTRI for a finite number of source exit temperatures.

$$Q = \dot{m}_h C_{ph}(150 - T_{exit}) \tag{12}$$

These values take into consideration the effect of heat flux on sub-cooled nucleate boiling region and flow boiling region. The flow boiling process is very complicated as, when the local heat flux reaches a critical heat flux (CHF), the wall starts becoming dry. Based on the region in which CHF is reached the drying out process is called Departure from nucleate boiling (DNB) or Dry-out, the former occurring at low dryness fraction and the latter at higher dryness fraction [10]. In the Matlab program, all geometrical parameters other than length were held constant and the heat transfer coefficient values for intermediate points was found by interpolation. The heat duty reduces along with the mass flow rate and mass flux as the source exit temperature is increased.
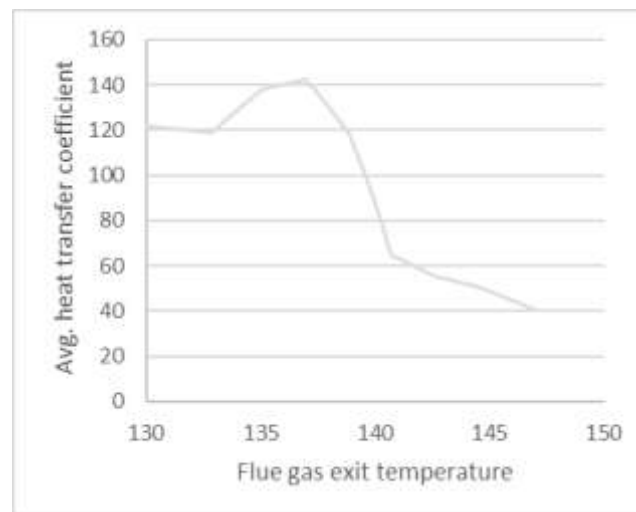
$$\dot{m}_c = \frac{Q}{(h_1 - h_4)} \tag{13}$$

The total length and that of the two phase portion and single phase portion was then found using the equations given below:

$$A_s = \frac{Q}{U_{eq} LMTD * Cf} \tag{14}$$

$$l = \frac{A_s}{N\pi d_o} \tag{15}$$

The values of tube side average heat transfer coefficient obtained are plotted against source exit temperature as shown below in fig. 6.

Fig. 6. Shows tube side average heat transfer coefficient versus flue gas exit temperature

The heat transfer coefficient for the flue gas was assumed to be constant since the free flow area in the shell remains unchanged and also because the variation in properties is minimum. It was found using McAdams correlation [9].

$$Nu = 0.36 Re^{0.55} Pr^{0.3} \tag{16}$$

$$h_{shell} = \frac{NuK}{D} \tag{17}$$

Equivalent heat transfer coefficient (Ueq) is calculated considering tube side average heat transfer, shell side heat transfer and conduction through the tube wall, in parallel.

IV. PRESSURE DROP EVALUATION IN EVAPORATOR

4.1 Shell Side

Bell Delaware method has been used to estimate the pressure drop due to friction. The pressure drop evaluation on the shell side of a shell and tube heat exchanger is complicated due to the presence of a cross-flow section, a window section and the inlet and exit sections. The total pressure drop is then the sum of the pressure drops for each window section and each cross-flow section, the number of such sections is decided by the number of baffles or baffle spacing. Empirical correlations for the total pressure drop including the cross-flow, window and the inlet-exit sections [8, 9] are:

$$\Delta p_s = \Delta p_{cr} + \Delta p_w + \Delta p_{i-o} = [(N_b - 1) \, \Delta p_b \varsigma_b + N_b \, \Delta p_w] \varsigma_l + 2 \, \Delta p_b \left(1 + \frac{N_{cw}}{N_{cc}}\right) \varsigma_b \varsigma_s$$

(18)

A Matlab program has been developed to obtain the pressure drop in the shell using the above equation. This was done after the total length of the heat exchanger was found in each iteration. In fig. 7 based on our process conditions and considering working fluid as R245fa the total pressure drop on shell side is obtained as 73.7Kpa at a source exit temperature of 127˚C. Pressure drop due to static head is also taken into account and the corresponding value obtained is 133Pa.
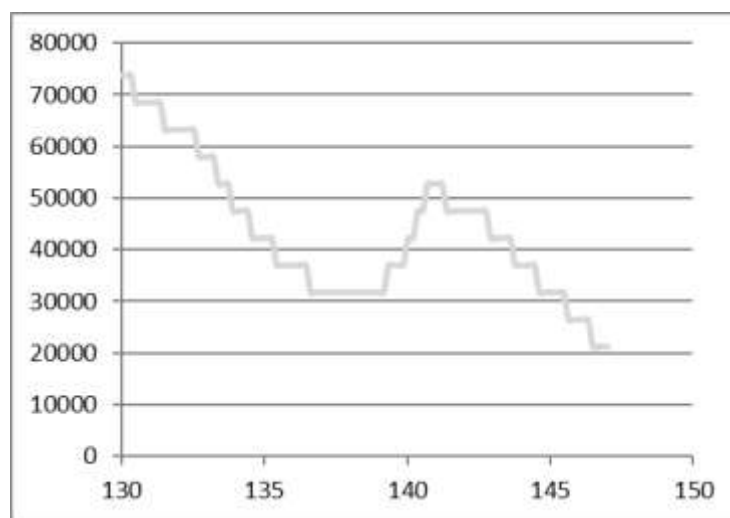

Fig. 7. Total shell side pressure drop with respect to source exit temperature

The step nature of the graph in fig. 7 is because the value of number of baffles can only be a whole number even though the length may vary continuously.

4.2 Tube Side (Single Phase)

The pressure drop inside the tubes is determined by using (19, 20):

$$\Delta p = \frac{G^2}{2\rho_i}\left[(1-\sigma^2+k_c)+2\left(\frac{\rho_i}{\rho_0}-1\right)+f\frac{L}{r_h}\rho_i\left(\frac{1}{\rho}\right)-(1-\sigma^2-k_e)\frac{\rho_i}{\rho_0}\right] \tag{19}$$

(entrance effect)   (momentum effect)   (core effect)   (exit effect)

Where, Fanning friction factor is:

$$f = (0.079)*Re^{-0.25} \tag{20}$$

The momentum pressure drop has been found to be negligible and has not been considered. Also the combined effect due to the pressure drop at the entrance and exit is very small and has hence been neglected. Hence the pressure drop in the core is the major contributor to the total tube side pressure drop. A Matlab program has been developed to obtain the pressure drop in tubes, with single phase consideration, using the above equations.

4.3 Tube Side (Two Phase)

For Pressure Drop calculations in tube side considering two phase the following pressure drop correlation [10] has been used:

$$\emptyset_{Lo}^2 = 1 + \frac{C}{X_{LM}} + \frac{1}{X_{LM}^2} \tag{21}$$

$$X_{LM} = \left(\frac{\rho_g}{\rho_l}\right)^{0.5}\left(\frac{\mu_l}{\mu_g}\right)^{0.1}\left(\frac{(1-x)}{x}\right)^{0.875} \tag{22}$$

$$\left(-\frac{d_p}{d_z}\right)_{fr} = \emptyset_{Lo}^2\left(-\frac{d_p}{d_z}\right)_{fr,Lo} \tag{23}$$

The term $\emptyset_{Lo}^2$ represents the two phase multiplier. The Lockhart- Martinelli method (21, 22) is among the oldest techniques. It assumes that the two phase multipliers are the functions of the Martinelli parameter equation as shown by (23). The phasic frictional gradients depend on the flow regimes of the phases, when each is assumed to flow alone in the channel. A Matlab program has been developed to obtain the pressure drop in tubes with two phase consideration using (21, 22 and 23).

The pressure drop on tube side due to friction (with combined single phase and two phase) is obtained as 4.25Pa for a source of temperature of 127˚C. It is observed that for increase in flue gas exit temperature the tube side pressure drop decreases. Pressure drop is a function of length of the tube and mass flux. In this case the mass flux continuously decreases with increase in flue gas exit temperature but the length fluctuates with respect to the same. The results in fig. 8 shows that the effect of mass flux dominates.
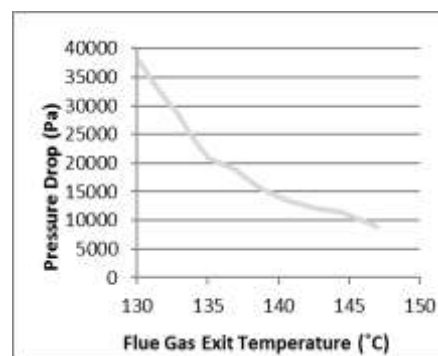

Fig. 8. Represents the total pressure drop in tube side for working fluid R245fa

Pressure drop due to static head has also been taken into account based on our process conditions and working fluid as R245fa.

V EXERGY DESTRUCTION IN THE EVAPORATOR CONSIDERING PRESSURE DROP

The procedure to calculate pressure drop in a shell and tube heat exchanger has been elucidated above. The exit state of the organic fluid in the evaporator is now calculated considering the pressure drop with respect to the inlet and taking the exit state to be saturated vapour (x=1).
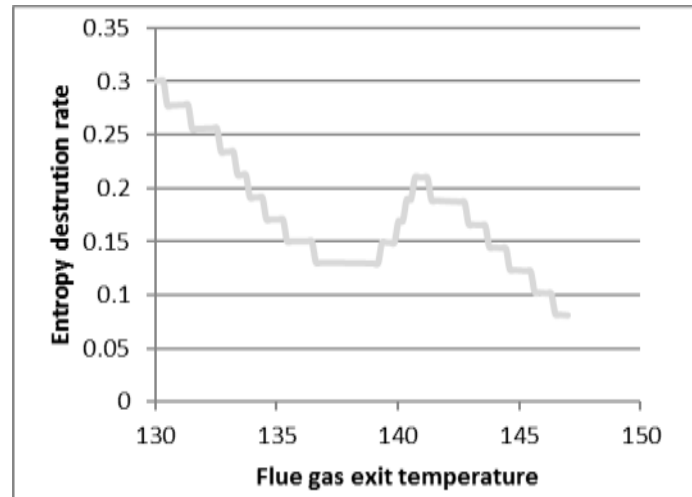
Fig. 9. Represents entropy destruction rate in evaporator versus flue gas exit temperature

The effect of pressure drop on the source exit temperature was not considered and the entropy at the exit was calculated after deducting the pressure drop from the inlet pressure. Comparing the exergy destruction due all three irreversibility's separately, we found that the pressure drop in the shell is the dominant contributor followed by the temperature difference in the evaporator and then the pressure drop in the tube, in descending order.

$$dS_{p,drop} = -\left(\frac{\partial v}{\partial T}\right) dF \qquad (24)$$

$$\alpha_v = \frac{1}{v\left(\frac{\partial v}{\partial T}\right)_p} \qquad (25)$$

Hence the total exergy destruction has a generally decreasing trend similar to that of pressure drop in shell, with a local minima and maxima. Yet for other heat sources with similar properties (volumetric thermal expansion coefficient) compared to the organic fluid, there might actually be more similar exergy destruction due to temperature difference and pressure drop and hence a trade-off may occur. Further it must be pointed out that there is a lot of flexibility in the rating procedure used, which will have a pronounced effect on the size of the heat exchanger and hence pressure drop. Finally the effect of the temperature difference in the evaporator must be highlighted, as the heat flux increases, sub-cooled nucleate boiling is enhanced along with the heat transfer coefficient but on further increase of heat flux, DNB occurs and the insulating vapour film along the inner periphery of the tube will result in a sharp decrease in heat transfer coefficient. This phenomena in-turn affects the length.

VI. CONCLUSION

- When the heat source parameters are fixed, the selection of the fluid should be based on the power output rather than the thermal efficiency. Maximum thermal efficiency was obtained for Toulene, R141b, D4, MDM, R245ca in decreasing order. Maximum power was obtained for Iso-Butane, Toluene, R236ea, R245fa in decreasing order. Hence even though the thermal efficiency for R245fa is considerably lower than the rest it has a high power output.

- Considering expansion in the turbine, at 85˚C, from 120˚C saturated condition, R125, R134a, R236ea had the lowest specific volumes in increasing order.

- Minimum overall exergy destruction (neglecting pressure drop in the evaporator) was obtained for R245fa, R245ca, R134a in increasing order. The fluids which had maximum power output, i.e. Iso-butane, Toluene and R236ea all had much higher overall exergy destruction. Hence a suitable weightage must be added to each parameter and the sum should be evaluated before selecting the fluid.

- It was found that the exergy destruction for R245fa due to pressure drop in the shell of the heat exchanger, was the much larger, even though the pressure drops are comparable on both sides. The partial derivative $\left(\frac{\partial v}{\partial T}\right)$ is very different for the flue gas and the organic fluid and the mass flow rate is very high. Hence the expected exergy trade-off was not found.

REFERENCES

[1] Z. Q. Wang, N. J. Guo and X. Y. Wang, Fluid selection and parametric optimization of organic rankine cycle for low temperature waste heat, Energy, 40, 2012, 107-115.

[2] Adrian Bejan, George Tsatsaronis and Michael Moran, Thermal Design and Optimization (John Wiley and Sons, Inc., NJ: Hoboken, 1996).

[3] Tzu-Chen Hung, Waste heat recovery of Organic Rankine Cycle using dry fluids, Energy Conversion and Management, 42, 2001, 539-553.

[4] Lars J. Brasz and William M. Bilbow, Ranking of working fluids for organic rankine cycle applications, International Refrigeration and Air Conditioning conference, 2004, 722-780.

[5] Yiping Dai, Jiangfeng Wang and Lin Gao, Parametric optimization and comparative study of organic rankine cycle (ORC) for low grade waste heat recovery, Energy Conversion and Management, 50, 2009, 576-582.

[6] J. Larjola, Electricity from industrial waste heat using high speed Organic Rankine Cycle (ORC), Production Economics, 41, 1995, 227-235.

[7] Donghong Wei, Xuesheng Lu, Zhen Lu and Jianming Gu, Performance analysis and optimization of organic Rankine cycle (ORC) for waste heat recovery, Energy Conversion and Management, 48, 2007, 1113–1119.

[8] Ramesh K. Shah and Dusan P. Sekulic, Fundamentals of heat exchanger design (John Wiley and Sons, Inc., NJ: Hoboken, 2003).

[9]   Sadic Kakac and Hongton Liu, Heat Exchangers: selection, rating and thermal design, 2nd ed (CRC Press,NJ: United States of America, 2002).

[10] S. Mostafa Ghiaasiaan, Two-Phase Flow, Boiling and Condensation in Conventional and Miniature Systems (Cambridge University Press, NJ: New York, 2008).